HHS Public Access

Author manuscript

J Immunol. Author manuscript; available in PMC 2021 February 09.

Published in final edited form as:

J Immunol. 2020 May 15; 204(10): 2697–2711. doi:10.4049/jimmunol.1901059.

Molecular Drivers of Lymphocyte Organization in Vertebrate Mucosal Surfaces: Revisiting the TNF Superfamily Hypothesis

Ryan D. Heimroth, **Elisa Casadei**, **Irene Salinas**

Center for Evolutionary and Theoretical Immunology, University of New Mexico, Albuquerque, NM 87131; and Department of Biology, University of New Mexico, Albuquerque, NM 87131

Abstract

The adaptive immune system of all jawed vertebrates relies on the presence of B and T cell lymphocytes that aggregate in specific body sites to form primary and secondary lymphoid structures. Secondary lymphoid organs include organized MALT (*O*-MALT) such as the tonsils and Peyer patches. *O*-MALT became progressively organized during vertebrate evolution, and the TNF superfamily of genes has been identified as essential for the formation and maintenance of *O*-MALT and other secondary and tertiary lymphoid structures in mammals. Yet, the molecular drivers of *O*-MALT structures found in ectotherms and birds remain essentially unknown. In this study, we provide evidence that TNFSFs, such as lymphotoxins, are likely not a universal mechanism to maintain *O*-MALT structures in adulthood of teleost fish, sarcopterygian fish, or birds. Although a role for TNFSF2 (TNF-α) cannot be ruled out, transcriptomics suggest that maintenance of *O*-MALT in nonmammalian vertebrates relies on expression of diverse genes with shared biological functions in neuronal signaling. Importantly, we identify that expression of many genes with olfactory function is a unique feature of mammalian Peyer patches but not the *O*-MALT of birds or ectotherms. These results provide a new view of *O*-MALT evolution in vertebrates and indicate that different genes with shared biological functions may have driven the formation of these lymphoid structures by a process of convergent evolution.

The development and organization of lymphoid tissues was a vital step in the evolution of the vertebrate immune system (1–3). Lymphoid organs can be classified into primary and secondary lymphoid organs (SLOs). Primary lymphoid organs are sites of lymphogenesis where lymphocyte progenitor cells differentiate into B and T lymphocytes. These sites include the bone marrow and the thymus in mammals, the thymus and bursa of Fabricius in birds and the thymus and head kidney in teleosts. SLOs are sites where immune cells interact with each other and immune responses are activated against foreign Ags. SLOs,

Address correspondence and reprint requests to Dr. Irene Salinas, Department of Biology, University of New Mexico, 167 Castetter Hall, MSC03-2020, Albuquerque, NM 87131-0001. isalinas@unm.edu.

Disclosures

The authors have no financial conflicts of interest.

The datasets presented in Supplemental Table II have been submitted to the National Center for Biotechnology Information (https://www.ncbi.nlm.nih.gov/bioproject/PRJNA4868500) under accession number PRJNA4868500. Lungfish TNF sequences have been submitted to the National Center for Biotechnology Information's GenBank (https://www.ncbi.nlm.nih.gov/genbank/) under accession numbers MK935171-MK935184 (African lungfish TNF super family), MK965520-MK965537 (African lungfish TNFR super family), and MN536217-MN536233 (South American TNF superfamily).

The online version of this article contains supplemental material.

such as the spleen, lymph nodes (LNs), and MALT, are therefore the birthplace of effective adaptive immune responses. SLO formation is genetically programmed, whereas tertiary lymphoid structures (TLS) are considered ectopic lymphoid accumulations that appear during adulthood in response to environmental stimuli (4).

MALT are immune inductive sites located at mucosal barriers that provide increased protection at areas of high pathogen encounter, allowing for efficient Ag trapping and rapid activation of the adaptive immune response. MALT includes diffuse MALT and organized MALT (*O*-MALT). Diffuse MALT consists of immune cells scattered throughout the epithelium acting as sentinels against invading pathogens and is present in all vertebrates from agnathans to mammals. *O*-MALT are composed of clusters of lymphocytes and can be found in both ectotherms and endo- therms. Similar to other SLOs, the *O*-MALT of endotherms is segregated into B and T cell zones, it contains follicular dendritic cells (FDCs) and the germinal center (GC) reaction allows for affinity maturation of the adaptive immune response via selection of high-affinity B cell clones. In ectotherms, however, little to modest affinity maturation can be detected, and SLOs do not have well-defined B and T cell zones (except for the spleen).

The evolutionary origins of *O*-MALT have long been a subject of debate among evolutionary immunologists. *O*-MALT was thought to have emerged in anuran amphibians as primitive lymphoid aggregates (LAs), but in 2015, primitive *O*-MALT structures were found in the gut and nasopharyngeal tissue of African lungfish (Sarcopterygii) (5) revealing that *O*-MALT is an innovation that predates the emergence of tetrapods. Lungfish LAs are thought to be SLOs because they were present in similar anatomical locations in all animals examined, and tertiary lymphoid organs (TLOs) coined as inducible LAs appeared in response to infection (5). Lungfish LAs share features with previously described LA in ectotherms because no compartmentalization into B and T cell zones or GCs were identified. Importantly, lungfish LAs are mostly composed of T cells and, to a lesser extent, B cells. Additionally, no evidence for somatic hypermutation was evident in lungfish Las, and therefore, the function of these structures remains enigmatic.

Although bona fide LAs are not present in teleost fish, a unique *O*-MALT-like structure known as interbranchial lymphoid tissue (ILT) has been reported in the gill arch of salmonids. The presence of ILT in Atlantic salmon is intriguing because no other lymphoid structures appear to be present in association with other teleost mucosal barriers such as the gastrointestinal tract. Similar to lungfish LAs and in contrast to mammalian SLOs, salmonid ILT mostly consists of diverse T cell clusters, shows high expression of CCL19, no expression of RAG-1, no B and T cell areas, and no GC formation (5–10). This is not surprising because GC reactions as defined in endotherms do not appear to occur in teleosts. Although salmon ILT is not present in yolk-sac larvae and first appears in juveniles (10), it is thought to be an SLO (10) and not a TLO because its localization and structure is similar in all individuals. In support, during infection, ILT decreases in size (8) rather than displaying the classical emergence of lymphocyte clusters at sites of inflammation associated with TLOs.

O-MALT evolution is also complex within endotherms. Birds, such as turkeys and chickens, do not possess LNs but do possess a pharyngeal tonsil, cecal tonsils (CT), and other *O*-MALT structures in their gastrointestinal tract that have a high level of organization, with FDCs that form part of the GCs (11–13). In birds, CT, similar to Peyer patches (PPs), develop during embryogenesis and therefore are present at birth (14). Despite the apparent similarity with mammalian SLOs, birds continue to surprise evolutionary immunologists because of the extensive reductionism of the immune gene repertoire in their genomes (12).

TNF superfamily (TNFSF) members play broad biological roles in cell proliferation, differentiation, inflammation, regulation of affinity maturation, and cell death (15–17). Additionally, TNFSF members are known for their importance in lymphoid tissue organogenesis and maintenance. Using several mouse knockout models (18–21), eight TNFSF members appear to be required for *O*-MALT formation, organization, maintenance, and function in mammals (15). Interestingly, TNFSF2 is found in all gnathos- tomes and some invertebrates (22), and lymphotoxins arose as a result of a gene the duplication process, as evidenced by the tandem arrangement in the human and mouse genomes and their high amino acid identity (23). Whereas knockout models of lymphotoxins and lymphotoxin receptors unequivocally indicate absence of organized SLOs (18, 24–26), TNFSF2/TNFRSF1A/1B knockout mice show very diverse phenotypes with respect to PP organogenesis (20, 21, 26–29).

In support to the TNFSF role in lymphoid development, several studies have suggested a progressive expansion of TNFSFs during vertebrate evolution, potentially explaining the progressive organization of lymphoid structures found from bony fish to mammals (5, 30). However, there are also lines of evidence against the TNFSF hypothesis. First, amphibians express TNFSF1 (LTA) and TNFSF3 (LTB); yet, their SLOs do not have GCs, and only modest levels of affinity maturation are observed (2, 31). Second, birds lack some TNFSFs that are vital for lymphocytic organization in mammals, such as TNFSF1 and TNFSF3 (13, 32) as well as other TNFSFs, such as TNFSF13 (APRIL) and TNFSF12 (TWEAK) (17). Thus, it appears that the function of lymphotoxins in amphibians is not the same as in mammals and that birds must use other mechanisms to generate and maintain *O*-MALT structures. Combined, these lines of evidence suggest that the molecular drivers of lymphocyte organization may be different in different vertebrate groups.

We hypothesize, in this study, that given the diversity of *O*-MALT structures and their different degrees of lymphocytic organization observed in vertebrates, these structures arose by convergent evolution creating lymphocytic aggregations of similar form but potentially different functions. As a consequence, whereas TNFSF may be essential for mammalian *O*-MALT formation and maintenance, alternative molecular drivers may be responsible for these processes in other vertebrate groups. To test this hypothesis, we use a comparative phylogenetic approach by performing RNA sequencing (RNA-Seq) of different *O*-MALT structures obtained from mammals, birds, sarcopterygian fish (lungfish), and bony fish, as well as in-depth analyses of TNFSF expression in the *O*-MALT in these four vertebrate groups. Our results support the notion that the TNFSF hypothesis likely does not explain the diversity of *O*-MALT structures present in vertebrates and provide a new model in which the

molecular drivers of *O*-MALT formation may require molecules involved in neuronal signaling.

Materials and Methods

Animals

Juvenile *Protopterus dolloi* (slender lungfish) (0.5 kg) were obtained from ExoticFishShop.com (https://exoticfishshop.net/) and maintained in 10- gallon aquarium tanks with dechlorinated water and a sand/gravel substrate, at a temperature of 27–29°C. Fish were acclimated to laboratory conditions for a minimum of 3 wk before being used for RNA-Seq. During this acclimation period, they were fed frozen earthworms once a day every third day. Feeding was terminated 48 h before the start of the experiment. A female preadult rainbow trout (200 g) was obtained from the Lisboa Springs Hatchery (Pecos, NM). A C57BL/6 adult female mouse (8–16 wk old) from The Jackson Laboratory (Bar Harbor, ME) was maintained at the Animal Research Facility of the University of New Mexico School of Medicine. Lungfish and trout were sacrificed with a lethal dose of Tricaine- S (MS-222; Thermo Fisher Scientific) with 200 mg/l water for 30 and 3 min, respectively. All animals used for this study were sampled between 9 and 11 AM. Each RNA-Seq library was prepared from tissues from one individual. All animal studies were reviewed and approved by the Office of Animal Care Compliance at the University of New Mexico (16–200384-MC, mouse protocol number 16–200497-HSC) and the United States Department of Agriculture, Beltsville Agriculture Research Center turkey protocol (number 17–008).

Tissue sampling

Lungfish nasal LAs were dissected as explained in (5). Adult rainbow trout ILT was dissected by scraping the lymphoid tissue located at the base of the gill arches. The trailing edge of the ILT was not included in the ILT tissue sample. Sterilely dissected mouse inguinal LNs and mouse PPs were generously donated by the Dr. J. Cannon Lab at the University of New Mexico School of Medicine. The turkey CT and turkey cecum from a 32- wk-old adult female turkey were provided by Dr. K. Krasnec at the United States Department of Agriculture. An adult Australian lungfish fin snip sample was kindly donated by Dr. M. Forstner. All samples were placed in RNAlater (Invitrogen, Thermo Fisher Scientific, Waltham, MA) and stored at — 80°C until processing.

Histology

For light microscopy, tissue samples from trout ILT, lungfish LA, turkey CT, and mouse PPs were fixed in 4% paraformaldehyde overnight, transferred to 70% ethanol, and embedded in paraffin ($n = 3$, except for turkey, $n = 2$). Samples were sectioned at a thickness of 5 mm, dewaxed in xylene, and stained using H&E for general morphological analysis. A total of six sections per sample were observed, and images were acquired with a Nikon Eclipse Ti-S Inverted Microscope and NIS-Elements Advanced Research Software (Version 4.20.02).

RNA-Seq and assembly

RNA from all tissues was extracted using TRIzol (Ambion, Life Technologies, Carlsbad, CA). Turbo DNAse (Invitrogen, Thermo Fisher Scientific) was used to remove any genomic

DNA contamination in the RNA. Illumina libraries were constructed using Kapa mRNA HyperPrep Kits (Roche Sequencing, Pleasanton, CA) and sequenced on an Illumina NextSeq 500 System platform at the University of New Mexico Molecular Biology Core Facility. Each library was generated with tissue from one individual. Sequence Read Archive (SRA) databases from the National Center for Biotechnology Information (NCBI) for trout muscle (DRR046645), turkey muscle (SRR478418), and mouse skin (SRR6884615) were downloaded as nonmucosal lymphoid tissue controls. The sratoolkit.2.9.0 fastq-dump was used to convert the SRAs into paired fastq files (33). The quality of the paired-end reads from our Illumina run and the SRAs were assessed using FastQC (34) and poor-quality reads were trimmed out using Trimmomattic set to default parameters (35). The trimmed reads were then assembled into de novo transcriptomes using Trinity (36, 37). The success of the assembly was assessed by realigning our raw fastq reads to the corresponding transcriptome using BWA (38) and samtools (39).

Data mining and TNFSF phylogenetic analysis

Published genomes for the representative species listed in Supplemental Table I were searched for TNFSF members in NCBI and Ensembl (40). To search for gene expression patterns in *O*-MALT from mouse, turkey, lungfish, and rainbow trout, TNFSF and TNFRSF protein sequences were downloaded from NCBI and used as queries for TBLASTN searches in our de novo-assembled transcriptomes (Supplemental Table II). A summary of transcriptome quality metrics is shown in Supplemental Table II. The resulting nucleotide sequences from these searches were used as queries for BLASTX searches in NCBI using hits with an E-value lower than or equal to 1×10^{-5}. Only the top hit for each search was used unless the top hit was an uncharacterized sequence, in which case the second hit, if characterized, was used. To ensure the detection of all distant TNF homologs, profile hidden Markov modeling (HMM) was implemented. To do this, our de novo transcriptomes were translated into protein databases with the longest open reading frame for each sequence using TransDecoder-5.0.0 (37) set with a minimum length of 100 aa. Raw HMM profiles for TNF (PF00229) and TNFR (PF00020) were downloaded from Pfam (41) and used in HMMER (http://hmmer.org/) to search our translated transcriptomes. Sequence alignments for TNFSF1, TNFSF2, and TNFRSF3 for all vertebrate classes were conducted using MAFFT, a multiple sequence alignment program (42). Selected TNF sequences were used to construct phylogenetic trees for ligands and receptors, respectively. Neighbor-joining phylogenetic trees were constructed using the Poisson correction with a bootstrap value of 1000 in MEGA X, as previously explained in (43) (Supplemental Figs. 1, 2).

To compare all the genes expressed in the generated transcriptomes, we first used DIAMOND (44) with the UniProt database (45). Resulting UniProt accession numbers from each transcriptome were then compared in Venny2.1 (46), and the common and unique accession numbers were used for gene ontology and KEGG pathway analysis using the DAVID bioinformatics database (47). Scatterplots identifying significant KEGG pathways ($p < 0.05$) were created in R (48).

Data availability

The datasets generated and/or analyzed during the current study are available in the NCBI under https://www.ncbi.nlm.nih.gov/bioproject/ PRJNA486850 (see Supplemental Table II). Lungfish TNF sequences were submitted to NCBI GenBank (African lungfish TNFSF accession numbers MK935171-MK935184, African lungfish TNFRSF accession numbers MK965520-MK965537, and South American TNFSF accession numbers MN536217-MN536233.

Results

Histological analysis of MALTs

As previously reported, histological examination of *O*-MALT in mice, turkey, African lungfish, and rainbow trout revealed the presence of poorly organized *O*-MALT in ectotherms, whereas highly organized *O*-MALT structures can be found in mice and turkeys (Fig. 1). Lungfish LAs have previously been reported to have a diameter between 300 and 350 μm (5). ILT was first discovered in salmon as lymphocytic accumulations at the base of each gill arch as well as a trailing edge to the distal end of the gill filament (9), and we also identified these structures in adult rainbow trout gill. Turkey CT and mouse PP have similar mean diameters of ~300 μm and, as previously reported, both of these structures showed a high degree of histological organization with defined compartmentalization into B and T cell zones (49, 50). Lungfish LA, as previously described (5), showed no compartmentalization, and it was composed of random clustering of lymphocytes with no distinct zones. Although we did not attempt to identify B and T cell zones in trout ILT in this study, these are not present in salmon ILT (9) or any other bony fish SLOs studied to date but are present in the spleen of cartilaginous fish (51).

Analysis of TNFSF and TNFRSF in vertebrate genomes

Bioinformatic analyses were performed among the major vertebrate classes to identify all TNFSF and TNFRSF genes with a focus on TNFSFs previously described as key factors in lymphoid tissue formation in mammals (Fig. 2A). Tacchi et al. (5) reported the presence of 18 TNF ligands and 27 TNFR in humans, 13 TNF ligands and nine TNFR in teleost, 14 TNF ligands and 15 TNFR in the coelacanth, and 13 TNF ligands and 14 TNFR in African lungfish. To revisit the TNFSF theory, we expanded our searches to include newly available genomes/transcriptomes for all vertebrate classes (Supplemental Table I). BLAST searches revealed the presence of 14 TNFSF ligands and 25 TNFSF receptors in teleost genomes. BALM was found in the newly sequenced teleost genomes, along with receptors TNFRSF1B, TNFRSF4, TNFRSF6B, TNFRSF7 (CD27), TNFRSF8, TNFRSF9, TNFRSF10B, TNFRSF11A, TNFRSF11B, TNFRSF12A, TNFRSF13B, TNFRSF14, TNFRSF18, TNFRSF19, and TNFRSF25 (Tables I, II). In coelacanth, BLAST searches did not reveal the presence of any new ligands but identified 10 more TNFR: TNFRSF1B, TNFRSF4, TNFRSF7, TNFRSF10B, TNFRSF11B, TNFRSF13B, TNFRSF17, TNFRSF18, TNFRSF25, and TNFRSF27. Searching all new African lungfish transcriptomes revealed the expression of ligands TNFSF9, TNFSF11, and BALM as well as receptors TNFRSF1B, TNFRSF8, TNFRSF12A, TNFRSF13C, and EDAR. In South American lungfish, our transcriptomes showed the expression of 10 ligands and 18 receptors. Amphibian and reptile

genomes showed the expression of 12 ligands and 21 receptors and 16 ligands and 24 receptors, respectively. The presence of 12 ligands and 27 receptors was detected in the bird genomes searched. As previously reported, TNFSF1, TNFSF3, and TNFRSF3 (LTBR) were absent from bird genomes (13) (Tables I, II). Finally, our searches confirmed all previously reported TNFSF molecules in human.

Because of the low sequence similarity between TNFSF molecules (52, 53), to identify distant TNFSF homologs we performed additional structural searches using HMM using the TNF homology domain (THD). HMM analyses revealed the presence of three more TNFR (TNFRSF4, TNFRSF8, and TNFRSF13C) in South American lungfish not found through BLAST searches. In African lung- fish, HMM searches identified the presence of one additional ligand, TNFSF9, and three additional receptors, TNFRSF EDAR, TNFRSF8, and TNFRSF9. HMM searches in trout, turkey, and mouse transcriptomes did not result in the identification of any novel TNFSFs or TNFRSFs (Tables I, II).

When focusing on the TNFs vital for lymphocyte organization in mice, we found that four of these molecules are evolution- arily conserved from bony fish to mammals, including TNFSF5 (CD40L), TNFRSF1A, TNFRSF5 (CD40), and TNFRSF11A. TNFSF1 and TNFSF3 showed complex evolutionary histories because they are present in the coelacanth but appear to be absent in Australian lungfish. The majority of tetrapods have TNFSF1 and TNFSF3 but they have been lost in Aves (54–56). Our analysis indicates that TNFRSF3 was lost in early tetrapods because it is present in bony fish and lungfish but not in amphibians. TNFRSF3 genes are found in mammals, suggesting deletion of TNFRSF3 in the amphibian lineage (Fig. 2A).

Phylogenetic analysis showed the homology between TNFSFs and TNFRSFs in bony vertebrates. TNFSF ligands mostly grouped within their respective family clade. In particular, within their clade, TNFSF ligands 10, 11, 5, 1, 2, 8, and 12 had bootstrap values higher than 50%. Hence, for these families, the lower sequence divergence may reflect a conservation of function. As expected, in lungfish, TNFSF ligands appeared more closely related to tetrapod TNFSF ligands compared with those of bony fish. TNFSF1 and TNFSF2 ligands shared a bootstrap value of 51%, with no clear separation among their members (Supplemental Fig. 1). As seen for some TNFSF, the phylogenetic tree for TNFRSFs showed that some receptor families are well conserved with bootstrap values higher than 50%. Specifically, the members of TNFRSF19, 19L, 27, EDAR, 16, 8, 21 and 11A families all appeared well conserved, with no clear separation among teleosts and other vertebrates. The only exception was salmon TNFRSF11A, which was more closely related to salmon and coelacanth TNFRSF5 than to other TNFRSF11A molecules. Interestingly, TNFRSF11B and 6 shared a bootstrap value of 75%, and their members appeared mixed within the two clades. Of particular relevance, we observed that in the majority of the TNFRSF clades, lungfish sequences appeared more closely related to those of teleosts than tetrapod counterparts (Supplemental Fig. 2).

TNFSF2, as predicted, was found in all scanned genomes/ transcriptomes (Fig. 2). As expected, the amino acid alignment of TNFSF2 molecules from representative vertebrate species showed high similarity among them as well as with the TNFSF1 family. Specifically,

several conserved amino acids were found in the 10 β-strands domains (A-H) present in human, with the highest degree of conservation observed in domain C (Fig. 3). Interestingly, the amino acid sequence of domain C in birds *(Gallus gallus)* showed several amino acid substitutions that deviate the TNFSF2 sequence considerably from that of mammals, amphibians, and lungfish. The corresponding receptors (TNFRSF1A and TNFRSF1B) were also found in all vertebrate groups, except for amphibians, in which surprisingly, TNFRSF1A is present but TNFRSF1B is missing (Table II).

These results provide a revised view of the complexity of TNFSF evolution in vertebrates and provide further support for the notion that SLOs emerged in each class of vertebrates in novel ways that are not always dependent on TNFSF members such as the lym- photoxin axis.

Expression of TNFSF and TNFRSF in ectotherm and endotherm O-MALT structures

Because of the lack of published lungfish genomes or tran- scriptomes obtained from *O*-MALT, we performed RNA-Seq on *O*-MALT tissues from mice, turkeys, African lungfish, and rainbow trout (Supplemental Table II). Searching these new transcriptomes indicated a similar expression pattern of TNFSFs as previously shown in Fig. 2A and 2B. Interestingly, we observed the expression of all TNFs vital to lymphoid tissue formation in mammals in the LA of the lungfish. Because a lungfish genome is not available, orthology assignment between lungfish and human TNFSF molecules can only be predicted based on the percentage of amino acid identity (57). Percentage amino acid identity analysis for TNFSF ligand and receptors present in both African lungfish and humans revealed that 17 out of the 32 molecules shared >30% sequence identity supporting orthology (58). Of the eight critical TNFs identified in mammalian studies (15), lungfish TNFSF1, TNFSF5, TNFSF11, and TNFRSF11 have >30% sequence identity with their human counterparts (Table III). The lower sequence identity of the remaining four members raises the question of whether they are involved in lymphoid organ development and organization. To gain some insights into this question, we performed amino acid sequence alignments and motif analyses of vertebrate TNFSF1 and TNFRSF3 molecules. Amino acid alignments for TNFSF1 showed the presence of the conserved THD in all jawed vertebrates. Additionally, this alignment confirmed that teleost TNF-new (TNFN) does not contain the conserved THD for TNFSF1, and therefore, it is not an ortholog of mammalian TNFSF1 (22) (Fig. 4). Similar to tetra-pods, lungfish TNFSF1 contained the conserved THD that makes up the typical jelly roll conformation of TNFs (52) and residues vital for binding TNFRSF3 were conserved in mammalian and African lungfish TNFSF1 sequences. In support of this, the percentage identity between human and African lungfish TNFSF1 was above 30% (Table III). Combined, this analysis suggests that lungfish TNFSF1 is an ortholog of mammalian TNFSF1. Although we did not perform amino acid sequence alignments for TNFSF3, the amino acid identity between lungfish and human TNFSF3 is ~27% (Table III), a value not sufficient to ascertain that the lungfish molecule carries out similar functions to the mammalian counterpart. Phylogenetic analysis showed that all vertebrate TNFSF3 molecules form one clade, whereas TNFSF1 molecules appear to be intermixed with TNFSF2 in a single clade, indicating that they are closely related.

TNFR do not contain a THD, but instead, are composed of short cysteine-rich domains (CRDs), which are essential for the interaction between TNSRSF3 and the TNFSF1 and TNFSF3 heterodimer (52). Amino acid alignment showed that CRDs are conserved in all the vertebrate TNFRSF3 molecules analyzed (Fig. 5A). The intracellular domain of TNFRSF3 contains both conventional and unconventional TRAF binding domains in coe- lacanth and tetrapods (59). However, teleost TNFRSF3 molecules, as well as African and South American lungfish TNFRSF3, lack these TRAF binding domains. Instead, teleost and South American lungfish have a bony fish-specific conserved TRAF binding motif, whereas the African lungfish does not (Fig. 5B). The lack of a TRAF binding motif suggests that African lungfish TNFRSF3 may not signal the same way as its mammalian counterpart and therefore may have an alternative function. In support, percentage identity analysis of TNFRSF3 sequences aligned in Fig. 5A and 5B show high sequence identity (66.98%) between the human and mouse sequences, whereas the percentage identity between human and African lungfish molecules is only 20.9%, indicating lack of orthology (Fig. 5C). This result supports the phylogenetic analysis findings that showed two separate clades for TNFRSF3, a clade containing teleost, lungfishes, and amphibian molecules and a second clade containing human, mouse, and coelacanth molecules (Supplemental Fig. 2).

As expected, we also noted the absence of TNFSF1, TNFSF3, or TNFRSF3 in turkey CT, as well as absence of TNFSF1 and TNFSF3 expression in rainbow trout, suggesting that alternative molecular mechanisms other than the lymphotoxin axis drive mucosal lymphoid tissue formation in birds and teleost fish. TNFSF2 transcripts were detected in all the *O*-MALT tran- scriptomes generated in this study, as well as the receptors TNFRSF1A and TNFRSF1B. Therefore, in the absence of the lymphotoxin axis, TNFSF2 may be driving the clustering of lymphocytes in nonmammalian species.

Unbiased search of molecular drivers of O-MALT structure in vertebrates

To elucidate previously unidentified molecular drivers and biological pathways involved in *O*-MALT formation, we compared the transcriptomes generated from four different *O*-MALT tissues from each representative vertebrate species. We obtained a total of 280,740 transcripts in the mouse PP transcriptome, 164,478 transcripts in the turkey CT transcriptome, 162,353 transcripts in the lungfish LA transcriptome, and 286,901 transcripts in the trout ILT transcriptome. We first removed genes expressed in negativecontrol tissue (nonlymphoid tissues) transcriptomes from each of the four species. This resulted in a total of 6483 transcripts for the mouse PP, 27,172 transcripts for turkey CT, 6772 transcripts for the lungfish LA, and 13,214 transcripts for the trout ILT. As illustrated by the Venn diagram, we observed few transcripts shared among all four *O*-MALT transcriptomes (Fig. 6). Turkey CT and trout ILT had the most transcripts in common with 3096 (6.9%), whereas mouse PP and lungfish LA had the lowest percentage of genes in common, with only 263 (0.6%). Turkey CT had the highest number of unique genes, with 20,520 (46%), whereas mouse PP and lungfish LA had a similar percentage of unique genes, with ~4000 (8.7–8.8%) each, and trout ILT had 8300 (18.6%) (Fig. 6).

We next performed gene ontology and KEGG pathway analysis of the respective gene lists that were unique or shared among *O*-MALTs (Fig. 7). Interestingly, genes unique to mouse

PPs were significantly enriched in genes belonging to olfactory transduction (Table IV). These included olfactory receptor (OR) family 8, subfamily B, member 4; OR family 2, subfamily H, member 1; and cyclic nucleotide gated channel β 1 (Table IV). To confirm these findings, we searched previously published SRAs from mouse inguinal LNs. We found that mouse LNs are also enriched in genes belonging to the olfactory transduction pathway, including OR families and cyclic nucleotide gated channels. Interestingly, 14 genes that were unique to lungfish LA were also enriched in the olfactory transduction KEGG pathway (Table IV). Additionally, we found a total of 97 genes that were unique to turkey CT and 20 genes that were unique to trout ILT that were enriched in the neuroactive ligand/receptor pathway. These included glycine receptors, cholinergic receptors, purinergic receptors, thyroid-stimulating hormone receptors, among others (Table V). When looking at genes shared between lungfish LA and turkey CT we found that they shared 12 genes that were enriched in the neuroactive ligand/receptor interaction pathway. Combined, our findings highlight little overlap in the transcriptome of different vertebrate *O*-MALT structures and unveil unique biological processes that likely drive lymphocyte aggregation in each vertebrate group, such as olfactory-related genes in mammals and sarcopterygian fish and neuronal-derived signals in birds and ectotherms.

Discussion

The organization of lymphocytes and other immune cells in discrete lymphoid structures is one of the hallmarks of the immune system of endotherms. This organization is believed to increase cell-Ag interactions, optimize Ag presentation and T cell stimulation, and lead to efficient selection of high-affinity B cell clones during the maturation of the immune response. SLOs, such as spleen, LNs, and *O*-MALT, develop during embryogenesis. In contrast, TLSs develop after birth and require chronic inflammation or microbial signals to develop. TLS include the isolated lymphoid follicles in the small intestine, the inducible bronchial- associated lymphoid tissue, and the TLS commonly associated with tumors (5, 60–62).

TNFSFs are vital molecules for the process of lymphoid tissue formation and organization in mammals (63). TNFSF molecules and signaling pathways govern both the formation of SLOs, such as the spleen, LNs, and PPs, as well as FDC, GC, and TLS (61–65). The current model for mammalian LN and PP formation relies on lymphoid tissue inducer (LTi) cells and an initial neuronal-derived signal (66). It has been proposed that retinoic acid released by the vagus nerve induces expression of CXCL13 by mesenchymal cells (66). However, evidence for the neuronal contributions to the initiation of this process are limited because only one previous study introduced this concept and follow-up experimental support is currently lacking. Precursor LTi cells start to cluster and signal through TNFSF11 and TNFRSF11, which initiates the expression of TNFSF1 and TNFSF3 on the precursor LTi cells that then become mature LTi cells. Mature LTi cells also rely on the lymphotoxin axis to initiate the expression of chemokines, adhesion molecules, and cytokines that facilitate the attraction and retention of more hematopoietic cells causing the growth and maintenance of the LN (63, 67–69). Thus, TNFRSF3-mediated signaling in response to the $LT\alpha_1\beta_2$ binding is the main pathway for promoting mammalian lymphoid tissue development. TNFSF1- deficient, TNFSF3-deficient, and TNFRSF3-deficient mice all have similar

defects during secondary and tertiary lymphoid organogenesis (70–72), whereas TNFSF2 deficiency results in diverse phenotypes, ranging from altered SLO morphology to no changes in SLO appearance, depending on the mouse model used (20, 21, 26–29). Specific differences in LN and PP organogenesis have, nevertheless, been reported (63). For instance, mice deficient in TNFRSF1A, a receptor for LT $\alpha_1\beta_2$, lack the formation of PPs but still retain LN development (21). Additionally, unlike LNs, PP formation requires a population of CD11c+ dendritic-like cells that express LT β and the receptor tyrosine kinase RET. Interestingly, RET was previously described as a neuroregulator (73–75), and innate lymphoid cells (ILCs) ILC3 in the gut express RET and respond to glial- derived neurotrophic factors (76). Additionally, PPs but not LNs are absent or significantly reduced in CXCL13- or CXCR5-deficient animals (77) as well as *sharpin-deficient* animals (78).

Despite the clear involvement of TNFSF molecules in mammalian SLO and TLS biology, it is still unclear whether TNFSFs also govern *O*-MALT formation and maintenance in ectotherms and whether these structures serve similar immunological functions to those described in mammals. The evolution of TNFSF and TNFRSF is very complex, and it involved small-scale duplications as well as large, genome-wide duplications (53). The coevolution of TNFSF and TNFRSF families is characterized by functional convergence, as evidenced by the fact that multiple ligands share the same receptor and that different ligand-receptor interactions can result in the same biological outcome (53). Of interest, *Drosophila* has one TNF ligand (Eiger) and one TNFR ligand (Wengen) (79), and *Drosophila* TNFSF molecules are highly expressed in the nervous system (80). We previously reported the expansion in TNFSF genes in African lungfish compared with other ectotherms and proposed that this expansion may explain the presence of *O*-MALT in lungfish (5). Since that study, new genomes and transcriptomes have become available, allowing us to revisit the TNFSF phylogeny. Additional structural searches also allowed us to refine our approaches that were previously limited to BLAST searches. Thus, in this study we report that TNFSF does not appear to have expanded in sarcopterygian fish because lower numbers of overall TNFSF genes were found in lungfish compared with bony fish. However, expansion of TNFs within teleosts may not be surprising, given the multiple genome duplication events that have occurred over bony fish evolution (81). *P. dolloi* is also a tetraploid species, and therefore, similar events could have contributed to TNFSF expansions in this lungfish species. Because of the lack of functional experiments at this point, it is unclear whether the TNFSF genes identified in ectotherms encode molecules with homologous functions to their mammalian counterparts, and further work is needed to clarify these questions.

Given the importance of the lymphotoxin axis that was revealed in murine studies, we focused on lymphotoxin sequence analyses in this study. TNFSF1 and TNFSF3 appear to be absent in teleost fish despite the fact that salmonids have ILT in their gills, a structure predominantly composed of T cells that lack the canonical B and T cell areas and GC formation found in endotherms (7, 9). In accord, previous efforts to discern teleost lymphotoxins showed that TNFRSF3 is present in teleosts but TNFSF1 and TNFSF3 are not. Teleost fish have a novel TNF, TNFN, that at first was considered to be the candidate homolog for mammalian lymphotoxins, but a recent study and our amino acid alignment showed that the structure and behavior of TNFN did not relate to either TNFSF1 or TNFSF3

(Fig. 4) (30, 59). Rather, TNFSF14 was found to bind to TNFRSF3, showing that, originally, TNFRSF3 was the receptor for TNFSF14. Recently, single-cell RNA-Seq analysis of RAG $^{-/-}$ zebrafish revealed the expression of ILC1-, ILC2-, and ILC3-type markers in zebrafish (82). Specifically, an ILC3-like cell subset found in zebrafish shares some transcriptional similarities to the mammalian LTi cells and exclusively expresses *tnfb* (TNFSF2), the ortholog to human LTa and a marker of LTi cells. Interestingly, we detected a partial contig for fish type I TNFSF2 in trout ILT by Illumina sequencing, and therefore, it is possible that TNFSF2 signaling alone is sufficient to drive lymphocytic aggregation in nonmammalian species. Because bony fish have two types of TNFSF2 (named I and II) (83), further studies are therefore required, for instance, to ascertain a role for each TNFSF2 gene in teleost ILT formation.

Amino acid sequence alignment of TNFRSF3 from jawed vertebrates showed that, whereas the extracellular domains are highly conserved, the transmembrane domain as well as the intracellular domain are not. Thus, the percentage identity at the amino acid level between *Protopterus* sp. TNFRSF3 and human TNFRSF3 is ~20%, a low value that suggests that these two molecules are not orthologs. This finding was further supported by the TNFRSF tree reported in this study (Supplemental Fig. 2). Functionally, our results suggest that TNFRSF3 signaling, as described in mammalian studies, may not occur in lungfish and further studies should investigate the biological function of lungfish TNFRSF3. Similarly, both amphibian and bony fish TNFRSF3 only shared a 20% amino acid identity with human TNFRSF3, indicating that ectotherm TNFRSF3 molecules may lack the signaling capabilities of their mammalian counterparts. Our findings, therefore, indicate that molecular signaling pathways other than the lym- photoxin pathway must be responsible for the formation and maintenance of teleost ILT and lungfish nasal *O*-MALT structures.

Although birds do not have LNs, they have *O*-MALT structures, such as CT and pharyngeal tonsils, that are structurally very similar to those found in mammals with FDCs and GCs (84). Mammalian studies have emphasized the importance of signaling through TNFRSF3 for lymphoid tissue formation, but the lack of the lymphotoxin axis in birds has not impeded their ability to form and maintain SLOs with a mammalian-like level of compart- mentalization (54). The loss of lymphotoxins in birds is not a rare event. Birds have the unique ability to compensate for losses in numerous immune genes/loci, including the Ig kappa L chain, peroxiredoxin, and other TNFSF members (15, 85–87). Thus, in agreement with previously published studies (32, 54), we found that bird genomes do not contain TNFSF1, TNFSF3, or TNFRSF3. Furthermore, our comparative transcriptomic data using turkey CT suggests that these structures may be generated by very different pathways in birds and mammals because no common gene expression signatures were found. Because we performed RNA-Seq analysis on *O*-MALT from adult animals, the gene expression patterns likely captured maintenance rather than organogenesis of this structure. Future studies should evaluate gene expression profiling during embryogenesis of bird SLOs to gain a deeper insight into the genes involved in their early organogenesis.

The interactions between the nervous system and the immune system are complex and bidirectional (88, 89). Along with TNFSFs, neurons have been proposed to produce metabolites such as retinoic acid that could contribute to SLO formation. In addition, a

subset of ILC3s are LTi-like cells characterized by the expression of retinoic acid-related orphan receptor γ T (ROR γ t), which are crucial initiators of SLO organogenesis (90). As mentioned earlier, ILC3 also expresses RET and responds to neurotrophic factors, providing additional evidence that neuronal signals may regulate SLO formation. Yet, this hypothesis has not been explored in other vertebrate groups, and experimental evidence is limited at this point. Our findings support a conserved role for neuronal-derived signals in SLO maintenance in adulthood. We found that neuroactive ligand and receptor pathways were enriched in trout, lungfish, turkey, and mouse SLO transcriptomic datasets. Among the genes identified in this pathway, we identified cholinergic receptors, dopamine receptors, γ -aminobutyric acid type A receptors, and cholinergic nicotinic receptors. Nicotinic acetylcholine receptors are present within SLOs, which are highly innervated with cholinergic fibers and have been shown to influence lymphocyte development (91). We found expression of five different γ -aminobutyric acid type A receptor a genes in turkey CT but not in other SLO transcriptomes examined. These receptors have been shown to affect a wide variety of immune processes, such as cytokine secretion, cell proliferation, phagocytic activity, and chemotaxis (92). Interestingly, we observed little overlap in the specific genes within this pathway expressed in each SLO, suggesting that neuronal functions rather than specific suites of genes guide SLO maintenance in different species. It is important to note that not all animals sampled in this study were the same age. Whereas African lungfish and trout tissues were obtained from juvenile/preadult stages, mouse and turkey samples were collected from adults. Thus, we cannot rule out that the gene expression patterns found in each SLO depend on the developmental stage as well as immunological and metabolic states at which each animal was sampled. Despite these caveats, we propose, in this study, that neuronal signals may guide the aggregation of T cells and B cells and the maintenance of SLO structures across vertebrates. Further studies are warranted to test this new paradigm.

OR genes are fast evolving genes and the largest gene family in mammalian genomes. In mice, 4% of all genes are olfactory genes, whereas in humans, olfactory genes make 1.4% of the genome (93). Although this expansion of OR genes in mammals is thought to reflect the importance of olfaction in the survival of this vertebrate group, ORs also play vital roles outside of the olfactory system and have widespread expression patterns (94, 95). For instance, OR ectopic expression is thought to be vital for cell-to-cell recognition, cell cycle, and migration in many cell types (96, 97). Additionally, odorant receptors regulate immune cell functions such as T cell migration and T cell accumulation in LNs (98) or chemotaxis of lung macrophages (99). The present study identified that both mammalian PPs, mammalian LNs, and lungfish LAs were significantly enriched in genes belonging to the olfactory transduction pathway. Because the lungfish LA we sampled was a nasal LA, we cannot rule out contamination of olfactory gene expression from connective tissue surrounding the LA, but contamination issues could not explain OR expression in mouse PPs or LNs. This observation is supported by the fact that ectopic expression of specific OR genes is high in mammalian lymphoid tissues. For instance, OR family 52, subfamily N, member 4 and OR family 56, subfamily B, member 1 expression is highest in human PPs out of 18 tissues measured (100) and OR 2A4 expression is highest in human LNs out of 33 tissues analyzed. Importantly, LTi cells express G protein-coupled receptor 183 (GPR183). This receptor is required for the formation of TLS such as cryptopatches and isolated lymphoid follicles

(90). In mice that are deficient in G protein ai2 subunit, PPs regress and colitis is observed, emphasizing the importance of G proteins in the formation and retention of SLO and TLS (101). Expression of OR genes in different subsets of immune cells within SLOs and TLS may allow for fast and specific mechanisms of cell-to-cell communication. Given the complexity, size, and evolutionary rates of the OR gene family in mammals, further work is warranted to define the nature of OR-mediated interactions within mammalian lymphoid structures.

In summary, our findings provide new insights into the molecules that drive the complexity and diversity of lymphocytic aggregates found at mucosal tissues of vertebrates. Exhaustive TNFSF phylogenetic studies indicate that, as suggested by others, this superfamily is not universally used by all vertebrates to achieve *O*-MALT formation and maintenance. We propose a new paradigm, in which genes with functions in neuroactive ligand and receptor interactions as well as olfactory-related genes may drive *O*-MALT maintenance in a group-specific manner. Although we do not provide functional evidence for this theory, our transcriptomic analyses suggest that neuronal inputs other than retinoic acid production are required for vertebrate SLO maintenance. Additionally, ectopic expression of olfactory genes appears to be a unique innovation of mammalian SLOs. Cooperation between olfactory genes and TNFSF members, particularly TNFSF2, may also occur and be critical for the structure and function of *O*-MALT. Further studies are warranted to confirm these new theories in this study proposed.

Supplementary Material

Refer to Web version on PubMed Central for supplementary material.

Acknowledgments

We thank Dr. Martin F. Flajnik for critical review of the manuscript and Dr. Lijing Bu for help with bioinformatics analysis. Dr. Judy Cannon provided mouse tissue samples, Dr. Katina Krasnec provided turkey tissue samples, and Dr. M. Forstner provided Australian lungfish tissue samples. We thank Dr. Amemiya for kindly sharing lungfish RNA-Seq datasets.

This work was supported by the National Institutes of Health/National Science Foundation Award 1456940 (to I.S.) and National Institutes of Health/Center for Evolutionary and Theoretical Immunology/Centers of Biomedical Research Excellence Grant P20GM103452.

Abbreviations used in this article

CRD	cysteine-rich domain
CT	cecal tonsil
FDC	follicular dendritic cell
GC	germinal center
HMM	hidden Markov modeling
ILC	innate lymphoid cell

ILT	interbranchial lymphoid tissue
LA	lymphoid aggregate
LN	lymph node
LTi	lymphoid tissue inducer
NCBI	National Center for Biotechnology Information
***O*-MALT**	organized MALT
OR	olfactory receptor
PP	Peyer patch
RNA-Seq	RNA sequencing
SLO	secondary lymphoid organ
SRA	Sequence Read Archive
THD	TNF homology domain
TLO	tertiary lymphoid organ
TLS	tertiary lymphoid structure
TNFN	TNF-new
TNFSF	TNF superfamily

References

1. Neely HR, and Flajnik MF. 2016 Emergence and evolution of secondary lymphoid organs. Annu. Rev. Cell Dev. Biol. 32: 693–711. [PubMed: 27362646]
2. Flajnik MF 2018 A cold-blooded view of adaptive immunity. Nat. Rev. Immunol. 18: 438–453. [PubMed: 29556016]
3. Zapata A, and Amemiya CT. 2000 Phylogeny of lower vertebrates and their immunological structures. Curr. Top. Microbiol. Immunol. 248: 67–107. [PubMed: 10793475]
4. Ruddle NH, and Akirav EM. 2009 Secondary lymphoid organs: responding to genetic and environmental cues in ontogeny and the immune response. J. Immunol. 183: 2205–2212. [PubMed: 19661265]
5. Tacchi L, Larragoite ET, Munoz P, Amemiya CT, and Salinas I. 2015 African lungfish reveal the evolutionary origins of organized mucosal lymphoid tissue in vertebrates. Curr. Biol. 25: 2417–2424. [PubMed: 26344090]
6. Bjørgen H, Løken OM, Aas IB, Fjelldal PG, Hansen T, Austbø L, and Koppang EO. 2019 Visualization of CCL19-like transcripts in the ILT, thymus and head kidney of Atlantic salmon (Salmo salar L.). Fish Shellfish Immunol. 93: 763–765. [PubMed: 31422180]
7. Haugarvoll E, Bjerkås I, Nowak BF, Hordvik I, and Koppang EO. 2008 Identification and characterization of a novel intraepithelial lymphoid tissue in the gills of Atlantic salmon. J. Anat. 213: 202–209. [PubMed: 19172734]
8. Aas IB,Austbø L, Konig M, Syed M, Falk K, Hordvik I, and Koppang EO. 2014 Transcriptional characterization of the T cell population within the sal- monid interbranchial lymphoid tissue. J. Immunol. 193: 3463–3469. [PubMed: 25172486]

9. Dalum AS, Austbø L, Bjørgen H, Skjødt K, Hordvik I, Hansen T, Fjelldal PG, C. M. Press, Griffiths DJ, and Koppang EO. 2015 The interbranchial lymphoid tissue of Atlantic Salmon (Salmo salar L) extends as a diffuse mucosal lymphoid tissue throughout the trailing edge of the gill filament. J. Morphol. 276: 1075–1088. [PubMed: 26011185]
10. Dalum AS, Griffiths DJ, Valen EC, Amthor KS, Austbo L, Koppang EO, C.M. Press, and Kvellestad A. 2016 Morphological and functional development of the interbranchial lymphoid tissue (ILT) in Atlantic salmon (Salmo salar L). Fish Shellfish Immunol. 58: 153–164. [PubMed: 27633679]
11. Oláh I, and Glick B. 1979 Structure of the germinal centers in the chicken caecal tonsil: light and electron microscopic and autoradiographic studies. Poult. Sci. 58: 195–210. [PubMed: 471885]
12. Crole MR, and Soley JT. 2012 Evidence of a true pharyngeal tonsil in birds: a novel lymphoid organ in *Dromaius novaehollandiae* and *Struthio camelus* (Palaeognathae). Front. Zool. 9: 21. [PubMed: 22909013]
13. Magor KE, Miranzo Navarro D, Barber MR, Petkau K, Fleming- Canepa X, Blyth GA, and Blaine AH. 2013 Defense genes missing from the flight division. Dev. Comp. Immunol. 41: 377–388. [PubMed: 23624185]
14. Kajiwara E, Shigeta A, Horiuchi H, Matsuda H, and Furusawa S. 2003 Development of Peyer's patch and cecal tonsil in gut-associated lymphoid tissues in the chicken embryo. J. Vet. Med. Sci. 65: 607–614. [PubMed: 12808213]
15. Das S, Sutoh Y, Hirano M, Han Q, Li J, Cooper MD, and Herrin BR. 2016 Characterization of lamprey BAFF-like gene: evolutionary implications. J. Immunol. 197: 2695–2703. [PubMed: 27543613]
16. Futterer A, Mink K, Luz A, Kosco-Vilbois MH, and Pfeffer K. 1998 The lymphotoxin beta receptor controls organogenesis and affinity maturation in peripheral lymphoid tissues. Immunity 9: 59–70. [PubMed: 9697836]
17. Pfeffer K 2003 Biological functions of tumor necrosis factor cytokines and their receptors. Cytokine Growth Factor Rev. 14: 185–191. [PubMed: 12787558]
18. De Togni P, Goellner J, Ruddle NH, Streeter PR, Fick A, Mariathasan S, Smith SC, Carlson R, Shornick LP, Strauss-Schoenberger J, et al. 1994 Abnormal development of peripheral lymphoid organs in mice deficient in lymphotoxin. Science 264: 703–707. [PubMed: 8171322]
19. Banks TA, Rouse BT, Kerley MK, Blair PJ, Godfrey VL, Kuklin NA, Bouley DM, Thomas J, Kanangat S, and Mucenski ML. 1995 Lymphotoxin- alpha-deficient mice. Effects on secondary lymphoid organ development and humoral immune responsiveness. J. Immunol. 155: 1685–1693. [PubMed: 7636227]
20. Pasparakis M, Alexopoulou L, Grell M, Pfizenmaier K, Bluethmann H, and Kollias G. 1997 Peyer's patch organogenesis is intact yet formation of B lymphocyte follicles is defective in peripheral lymphoid organs of mice deficient for tumor necrosis factor and its 55-kDa receptor. Proc. Natl. Acad. Sci. USA 94: 6319–6323. [PubMed: 9177215]
21. Neumann B, Luz A, Pfeffer K, and Holzmann B. 1996 Defective Peyer's patch organogenesis in mice lacking the 55-kD receptor for tumor necrosis factor. J. Exp. Med. 184: 259–264. [PubMed: 8691140]
22. Wiens GD, and Glenney GW. 2011 Origin and evolution of TNF and TNF receptor superfamilies. Dev. Comp. Immunol. 35: 1324–1335. [PubMed: 21527275]
23. Cuff CA, and Ruddle NH. 1998 Lymphotoxin In Encyclopedia of Immunology. Delves PJ, and Roitt I, eds. Academic Press, London, p. 1637–1641.
24. Liepinsh DJ, Grivennikov SI, Klarmann KD, Lagarkova MA, Drutskaya MS, Lockett SJ, Tessarollo L, McAuliffe M, Keller JR, Kuprash DV, and Nedospasov SA. 2006 Novel lymphotoxin alpha (LTalpha) knockout mice with unperturbed tumor necrosis factor expression: reassessing LTalpha biological functions. Mol. Cell. Biol. 26: 4214–4225. [PubMed: 16705172]
25. Ying X, Chan K, Shenoy P, Hill M, and Ruddle NH. 2005 Lymphotoxin plays a crucial role in the development and function of nasal-associated lymphoid tissue through regulation of chemokines and peripheral node addressin. Am. J. Pathol. 166: 135–146. [PubMed: 15632007]
26. Ruddle NH 2014 Lymphotoxin and TNF: how it all began-a tribute to the travelers. Cytokine Growth Factor Rev. 25: 83–89. [PubMed: 24636534]

27. Tumanov AV, Grivennikov SI, Kruglov AA, Shebzukhov YV, Koroleva EP, Piao Y, Cui CY, Kuprash DV, and Nedospasov SA. 2010 Cellular source and molecular form of TNF specify its distinct functions in organization of secondary lymphoid organs. Blood 116: 3456–3464. [PubMed: 20634375]
28. Korner H, Riminton DS, Strickland DH, Lemckert FA, Pollard JD, and Sedgwick JD. 1997 Critical points of tumor necrosis factor action in central nervous system autoimmune inflammation defined by gene targeting. J. Exp. Med. 186: 1585–1590. [PubMed: 9348316]
29. Kuprash DV, Tumanov AV, Liepinsh DJ, Koroleva EP, Drutskaya MS, Kruglov AA, Shakhov AN, Southon E, Murphy WJ, Tessarollo L, et al. 2005 Novel tumor necrosis factor-knockout mice that lack Peyer's patches. Eur. J. Immunol. 35: 1592–1600. [PubMed: 15832287]
30. Glenney GW, and Wiens GD. 2007 Early diversification of the TNF superfamily in teleosts: genomic characterization and expression analysis. J. Immunol. 178: 7955–7973. [PubMed: 17548633]
31. Hofmann J, Greter M, Du Pasquier L, and Becher B. 2010 B-cells need a proper house, whereas T-cells are happy in a cave: the dependence of lymphocytes on secondary lymphoid tissues during evolution. Trends Immunol. 31: 144–153. [PubMed: 20181529]
32. Kaiser P 2012 The long view: a bright past, a brighter future? Forty years of chicken immunology pre- and post-genome. Avian Pathol. 41: 511–518. [PubMed: 23237363]
33. Sequence Read Archive Submissions Staff. 2011 Understanding SRA search results In SRA Knowledge Base. National Center for Biotechnology Information (US), Bethesda, MD Available at: https://www.ncbi.nlm.nih.gov/books/NBK56913/ Accessed: October 10, 2018.
34. Andrews S 2010 FastQC: a quality control tool for high throughput sequence data. Available at: http://www.bioinformatics.babraham.ac.uk/projects/fastqc Accessed: October 10, 2018.
35. Bolger AM, Lohse M, and Usadel B. 2014 Trimmomatic: a flexible trimmer for Illumina sequence data. Bioinformatics 30: 2114–2120. [PubMed: 24695404]
36. Grabherr MG, Haas BJ, Yassour M, Levin JZ, Thompson DA, Amit I, Adiconis X, Fan L, Raychowdhury R, Zeng Q, et al. 2011 Full-length transcriptome assembly from RNA-seq data without a reference genome. Nat. Biotechnol. 29: 644–652. [PubMed: 21572440]
37. Haas BJ, Papanicolaou A, Yassour M, Grabherr M, Blood PD, Bowden J, Couger MB, Eccles D, Li B, Lieber M, et al. 2013 De novo transcript sequence reconstruction from RNA-seq using the Trinity platform for reference generation and analysis. Nat. Protoc. 8: 1494–1512. [PubMed: 23845962]
38. Li H, and Durbin R. 2009 Fast and accurate short read alignment with Burrows-Wheeler transform. Bioinformatics 25: 1754–1760. [PubMed: 19451168]
39. Li H, Handsaker B, Wysoker A, Fennell T, Ruan J, Homer N, Marth G, Abecasis G, and Durbin R, 1000 Genome Project Data Processing Subgroup. 2009. The sequence alignment/map format and SAMtools. Bioinformatics 25: 2078–2079.
40. Zerbino DR, Achuthan P, Akanni W, Amode MR, Barrell D, Bhai J, Billis K, Cummins C, Gall A, Giron CG, et al. 2018 Ensembl 2018. Nucleic Acids Res. 46: D754–D761. [PubMed: 29155950]
41. Finn RD, Coggill P, Eberhardt RY, Eddy SR, Mistry J, Mitchell AL, Potter SC, Punta M, Qureshi M, Sangrador-Vegas A, et al. 2016 The Pfam protein families database: towards a more sustainable future. Nucleic Acids Res. 44: D279–D285. [PubMed: 26673716]
42. Katoh K, and Standley DM. 2013 MAFFT multiple sequence alignment software version 7: improvements in performance and usability. Mol. Biol. Evol. 30: 772–780. [PubMed: 23329690]
43. Kumar S, Stecher G, Li M, Knyaz C, and Tamura K. 2018 MEGA X: molecular evolutionary genetics analysis across computing platforms. Mol. Biol. Evol. 35: 1547–1549. [PubMed: 29722887]
44. Buchfink B, Xie C, and Huson DH. 2015 Fast and sensitive protein alignment using DIAMOND. Nat. Methods 12: 59–60. [PubMed: 25402007]
45. Chen C, Huang H, and Wu CH. 2017 Protein bioinformatics databases and resources. Methods Mol. Biol. 1558: 3–39. [PubMed: 28150231]
46. Oliveros JC 2015 Venny. An interactive tool for comparing lists with Venn's diagrams. Available at: http://bioinfogp.cnb.csic.es/tools/venny/index.html Accessed: March 12, 2018.

47. Huang DW, Sherman BT, and Lempicki RA. 2009 Systematic and integrative analysis of large gene lists using DAVID bioinformatics resources. Nat. Protoc. 4: 44–57. [PubMed: 19131956]
48. R Core Team. 2017 R: A Language and Environment for Statistical Computing. R Foundation for Statistical Computing, Vienna, Austria Available at: www.R-project.org/ Accessed: February 12, 2017.
49. Jung C, Hugot JP, and Barreau F. 2010 Peyer's patches: the immune sensors of the intestine. Int. J. Inflamm. 2010: 823710.
50. Rezaian M, and Hamedi S. 2007 Histological study of the caecal tonsil in the cecum of 4– 6 months of age white leghorn chicks. Am. J. Anim. Vet. Sci. 2: 5054.
51. Rumfelt LL, McKinney EC, Taylor E, and Flajnik MF. 2002 The development of primary and secondary lymphoid tissues in the nurse shark Ginglymostoma cirratum: B-cell zones precede dendritic cell immigration and T-cell zone formation during ontogeny of the spleen. Scand. J. Immunol. 56: 130–148. [PubMed: 12121433]
52. Bodmer JL, Schneider P, and Tschopp J. 2002 The molecular architecture of the TNF superfamily. Trends Biochem. Sci. 27: 19–26. [PubMed: 11796220]
53. Collette Y, Gilles A, Pontarotti P, and Olive D. 2003 A co-evolution perspective of the TNFSF and TNFRSF families in the immune system. Trends Immunol. 24: 387–394. [PubMed: 12860530]
54. Kaiser P, Poh TY, Rothwell L, Avery S, Balu S, Pathania US, Hughes S, Goodchild M, Morrell S, Watson M, et al. 2005 A genomic analysis of chicken cytokines and chemokines. J. Interferon Cytokine Res. 25: 467–484. [PubMed: 16108730]
55. Dalloul RA, Long JA, Zimin AV, Aslam L, Beal K, Blomberg Le Ann P, Bouffard P, Burt DW, Crasta O, Crooijmans RP, et al. 2010 Multiplatform next-generation sequencing of the domestic Turkey (Meleagris gal- lopavo): genome assembly and analysis. PLoS Biol. 8: e1000475. [PubMed: 20838655]
56. Barreda DR, Neely HR, and Flajnik MF. 2016 Evolution of myeloid cells. Microbiol. Spectr. DOI: 10.1128/microbiolspec.MCHD-0007-2015.
57. van Noort V, Snel B, and Huynen MA. 2003 Predicting gene function by conserved co-expression. Trends Genet. 19: 238–242. [PubMed: 12711213]
58. Rost B 1999 Twilight zone of protein sequence alignments. Protein Eng. 12: 85–94. [PubMed: 10195279]
59. Maeda T, Suetake H, Odaka T, and Miyadai T. 2018 Original ligand for LT^R is LIGHT: insight into evolution of the LT/LT βR system. J. Immunol. 201: 202–214. [PubMed: 29769272]
60. Lorenz RG, Chaplin DD, McDonald KG, McDonough JS, and Newberry RD. 2003 Isolated lymphoid follicle formation is inducible and dependent upon lymphotoxin-sufficient B lymphocytes, lymphotoxin beta receptor, and TNF receptor I function. J. Immunol. 170: 5475–5482. [PubMed: 12759424]
61. Drayton DL, Liao S, Mounzer RH, and Ruddle NH. 2006 Lymphoid organ development: from ontogeny to neogenesis. Nat. Immunol. 7: 344–353. [PubMed: 16550197]
62. Buckley CD, Barone F, Nayar S, Bénézech C, and Caamaño J. 2015 Stromal cells in chronic inflammation and tertiary lymphoid organ formation. Annu. Rev. Immunol. 33: 715–745. [PubMed: 25861980]
63. van de Pavert SA, and Mebius RE. 2010 New insights into the development of lymphoid tissues. Nat. Rev. Immunol. 10: 664–674. [PubMed: 20706277]
64. Ager A 2017 High endothelial venules and other blood vessels: critical regulators of lymphoid organ development and function. Front. Immunol. 8: 45. [PubMed: 28217126]
65. Finke D, and Kraehenbuhl JP. 2001 Formation of Peyer's patches. Curr. Opin. Genet. Dev. 11: 561–567. [PubMed: 11532399]
66. van de Pavert SA, Olivier BJ, Goverse G, Vondenhoff MF, Greuter M, Beke P, Kusser K, Hopken UE, Lipp M, Niederreither K, et al. 2009 Chemokine CXCL13 is essential for lymph node initiation and is induced by retinoic acid and neuronal stimulation. Nat. Immunol. 10: 1193–1199. [PubMed: 19783990]
67. Hehlgans T, and Pfeffer K. 2005 The intriguing biology of the tumour necrosis factor/tumour necrosis factor receptor superfamily: players, rules and the games. Immunology 115: 1–20. [PubMed: 15819693]

68. Upadhyay V, and Fu YX. 2014 Lymphotoxin organizes contributions to host defense and metabolic illness from innate lymphoid cells. Cytokine Growth Factor Rev. 25: 227–233. [PubMed: 24411493]
69. Onder L, and Ludewig B. 2018 A fresh view on lymph node organogenesis. Trends Immunol. 39: 775–787. [PubMed: 30150089]
70. Matsumoto M, Fu YX, Molina H, Huang G, Kim J, Thomas DA, Nahm MH, and Chaplin DD. 1997 Distinct roles of lymphotoxin a and the type I tumor necrosis factor (TNF) receptor in the establishment of follicular dendritic cells from non-bone marrow-derived cells. J. Exp. Med. 186: 1997–2004. [PubMed: 9396768]
71. Mounzer RH, Svendsen OS, Baluk P, Bergman CM, Padera TP, Wiig H, Jain RK, McDonald DM, and Ruddle NH. 2010 Lymphotoxin- alpha contributes to lymphangiogenesis. Blood 116: 2173–2182. [PubMed: 20566898]
72. Upadhyay V, and Fu YX. 2013 Lymphotoxin signalling in immune homeostasis and the control of microorganisms. Nat. Rev. Immunol. 13: 270–279. [PubMed: 23524463]
73. Sugaya R, Ishimaru S, Hosoya T, Saigo K, and Emori Y. 1994 A Drosophila homolog of human proto-oncogene ret transiently expressed in embryonic neuronal precursor cells including neuroblasts and CNS cells. Mech. Dev. 45: 139–145. [PubMed: 8199050]
74. Soba P, Han C, Zheng Y, Perea D, Miguel-Aliaga I, Jan LY, and Jan YN. 2015 The Ret receptor regulates sensory neuron dendrite growth and integrin mediated adhesion. eLife.
75. Perea D, Guiu J, Hudry B, Konstantinidou C, Milona A, Hadjieconomou D, Carroll T, Hoyer N, Natarajan D, Kallijarvi J, et al. 2017 Ret receptor tyrosine kinase sustains proliferation and tissue maturation in intestinal epithelia. EMBO J. 36: 3029–3045. [PubMed: 28899900]
76. Ibiza S, Garcia-Cassani B, Ribeiro H, Carvalho T, Almeida L, Marques R, Misic AM, Bartow-McKenney C, Larson DM, Pavan WJ, et al. 2016 Glial-cell-derived neuroregulators control type 3 innate lymphoid cells and gut defence. Nature 535: 440–443. [PubMed: 27409807]
77. Velaga S, Herbrand H, Friedrichsen M, Jiong T, Dorsch M, Hoffmann MW, Förster R, and Pabst O. 2009 Chemokine receptor CXCR5 supports solitary intestinal lymphoid tissue formation, B cell homing, and induction of intestinal IgA responses. J. Immunol. 182: 2610–2619. [PubMed: 19234155]
78. Seymour R, Shirley B-J, HogenEsch H, Shultz LD, and Sundberg JP. 2013 Loss of function of the mouse sharpin gene results in Peyer's patch regression. PLoS One 8: e55224. [PubMed: 23424624]
79. Kanda H, Igaki T, Kanuka H, Yagi T, and Miura M. 2002 Wengen, a member of the Drosophila tumor necrosis factor receptor superfamily, is required for Eiger signaling. J. Biol. Chem. 277: 28372–28375. [PubMed: 12084706]
80. Igaki T, Kanda H, Yamamoto-Goto Y, Kanuka H, Kuranaga E, Aigaki T, and Miura M. 2002 Eiger, a TNF superfamily ligand that triggers the Drosophila JNK pathway. EMBO J. 21: 3009–3018. [PubMed: 12065414]
81. Ravi V, and Venkatesh B. 2018 The divergent genomes of teleosts. Annu. Rev. Anim. Biosci. 6: 47–68. [PubMed: 29447475]
82. Hernández PP, Strzelecka PM, Athanasiadis EI, Hall D, Robalo AF, Collins CM, Boudinot P, Levraud JP, and Cvejic A. 2018 Single-cell transcriptional analysis reveals ILC-like cells in zebrafish. Sci. Immunol. 3: eaau5265. [PubMed: 30446505]
83. Hong S, Li R, Xu Q, Secombes CJ, and Wang T. 2013 Two types of TNF-a exist in teleost fish: phylogeny, expression, and bioactivity analysis of type-II TNF-α3 in rainbow trout Oncorhynchus mykiss. J. Immunol. 191: 5959–5972. [PubMed: 24244011]
84. Nagy N, and Olah I. 2007 Pyloric tonsil as a novel gut-associated lymphoepithelial organ of the chicken. J. Anat. 211: 407–411. [PubMed: 17593219]
85. Das S, Nikolaidis N, Klein J, and Nei M. 2008 Evolutionary redefinition of immunoglobulin light chain isotypes in tetrapods using molecular markers. Proc. Natl. Acad. Sci. USA 105: 16647–16652. [PubMed: 18940927]
86. Das S, Mohamedy U, Hirano M, Nei M, and Nikolaidis N. 2010 Analysis of the immunoglobulin light chain genes in zebra finch: evolutionary implications. Mol. Biol. Evol. 27: 113–120. [PubMed: 19744999]

87. Pirson M, Clippe A, and Knoops B. 2018 The curious case of peroxiredoxin- 5: what its absence in aves can tell us and how it can be used. BMC Evol. Biol. 18: 18. [PubMed: 29422028]

88. Wrona D 2006 Neural-immune interactions: an integrative view of the bidirectional relationship between the brain and immune systems. J. Neuroimmunol. 172: 38–58. [PubMed: 16375977]

89. Aballay A 2013 Role of the nervous system in the control of proteostasis during innate immune activation: insights from C. elegans. PLoS Pathog. 9: e1003433. [PubMed: 23950707]

90. Emgård J, Kammoun H, Garcia-Cassani B, Chesné J, Parigi SM, Jacob JM, Cheng HW, Evren E, Das S, Czarnewski P, et al. 2018 Oxysterol sensing through the receptor GPR183 promotes the lymphoid-tissue- inducing function of innate lymphoid cells and colonic inflammation. Immunity 48: 120–132.e8. [PubMed: 29343433]

91. Skok M, Grailhe R, Agenes F, and Changeux JP. 2006 The role of nicotinic acetylcholine receptors in lymphocyte development. J. Neuroimmunol. 171: 86–98. [PubMed: 16253349]

92. Mendu SK, Bhandage A, Jin Z, and Birnir B. 2012 Different subtypes of GABA-A receptors are expressed in human, mouse and rat T lymphocytes. PLoS One 7: e42959. [PubMed: 22927941]

93. Godfrey PA, Malnic B, and Buck LB. 2004 The mouse olfactory receptor gene family. Proc. Natl. Acad. Sci. USA 101: 2156–2161. [PubMed: 14769939]

94. Feldmesser E, Olender T, Khen M, Yanai I, Ophir R, and Lancet D. 2006 Widespread ectopic expression of olfactory receptor genes. BMC Genomics 7: 121. [PubMed: 16716209]

95. MaBberg D, and Hatt H. 2018 Human olfactory receptors: novel cellular functions outside of the nose. Physiol. Rev. 98: 1739–1763. [PubMed: 29897292]

96. Zhang X, and Eggert US. 2013 Non-traditional roles of G protein-coupled receptors in basic cell biology. Mol. Biosyst. 9: 586–595. [PubMed: 23247090]

97. Tsai T, Veitinger S, Peek I, Busse D, Eckardt J, Vladimirova D, Jovancevic N, Wojcik S, Gisselmann G, Altmüller J, et al. 2017 Two olfactory receptors-OR2A4/7 and OR51B5-differentially affect epidermal proliferation and differentiation. Exp. Dermatol. 26: 58–65. [PubMed: 27315375]

98. Clark AA, Nurmukhambetova S, Li X, Munger SD, and Lees JR. 2016 Odorants specifically modulate chemotaxis and tissue retention of CD4+ T cells via cyclic adenosine monophosphate induction. J. Leukoc. Biol. 100: 699–709. [PubMed: 27154353]

99. Li JJ, Tay HL, Plank M, Essilfie AT, Hansbro PM, Foster PS, and Yang M. 2013 Activation of olfactory receptors on mouse pulmonary macrophages promotes monocyte chemotactic protein-1 production. PLoS One 8: e80148. [PubMed: 24278251]

100. Bastian F, Parmentier G, Roux J, Moretti S, Laudet V, and Robinson- Rechavi M. 2008 Bgee: integrating and comparing heterogeneous transcriptome data among species. Lect. Notes Comput. Sci. 5109: 124–131.

101. Ohman L, Franzen L, Rudolph U, Birnbaumer L, and Hornquist EH. 2002 Regression of Peyer's patches in G a i2 deficient mice prior to colitis is associated with reduced expression of Bcl-2 and increased apoptosis. Gut 51: 392–397. [PubMed: 12171962]

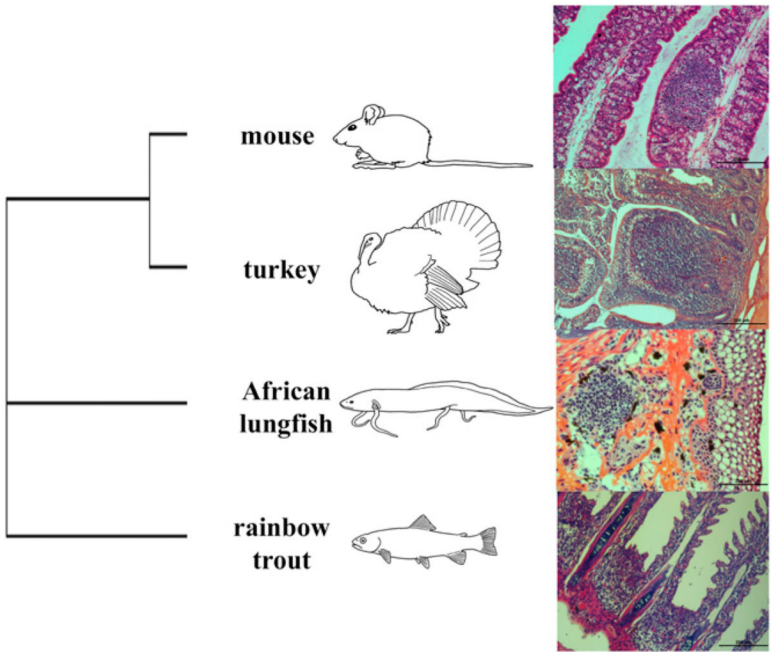

FIGURE 1.

Phylogenetic representation of *O*-MALT formation in bony jawed vertebrates (right) and light microscopy images of H&E-stained sections from the different *O*-MALT structures used in this study.

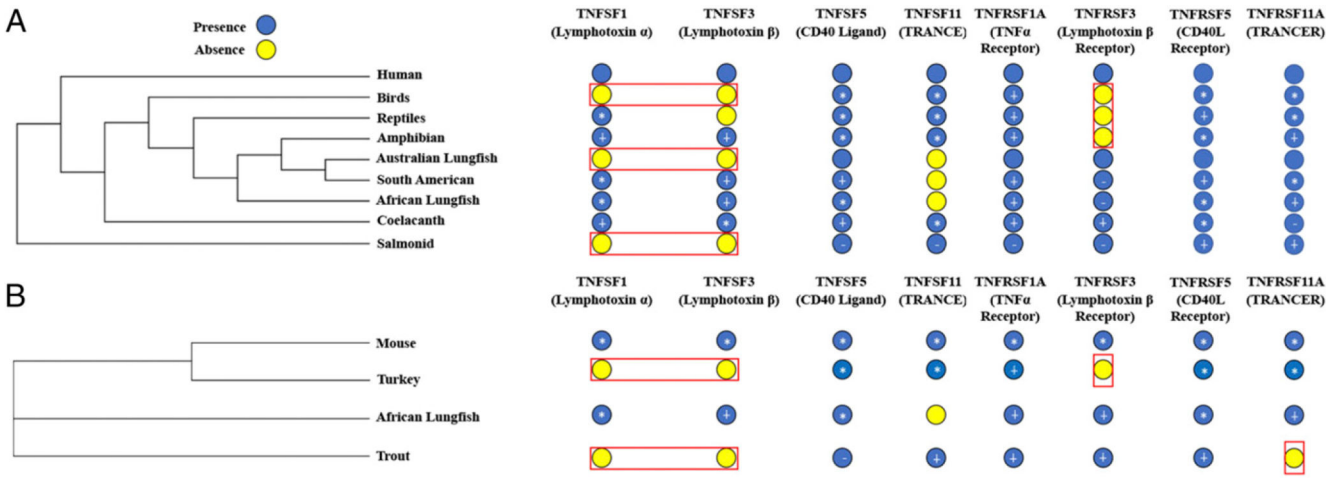

FIGURE 2.

Expression of TNFs vital to secondary lymphoid tissue formation in vertebrates. (**A**) Expression of TNFs in previously published genomes and transcriptomes. (**B**) Expression of TNFs in *O*-MALT sequenced from mouse PP, turkey CT, African lungfish LA, and trout ILT. *, an amino acid percentage identity with human ≥30%; +, amino an acid percentage identity with human between 30 and 20%; —, amino acid percentage identity with human of <20%. The red boxes denote important TNFs for secondary lymphoid tissue development that were absent in searched genomes.

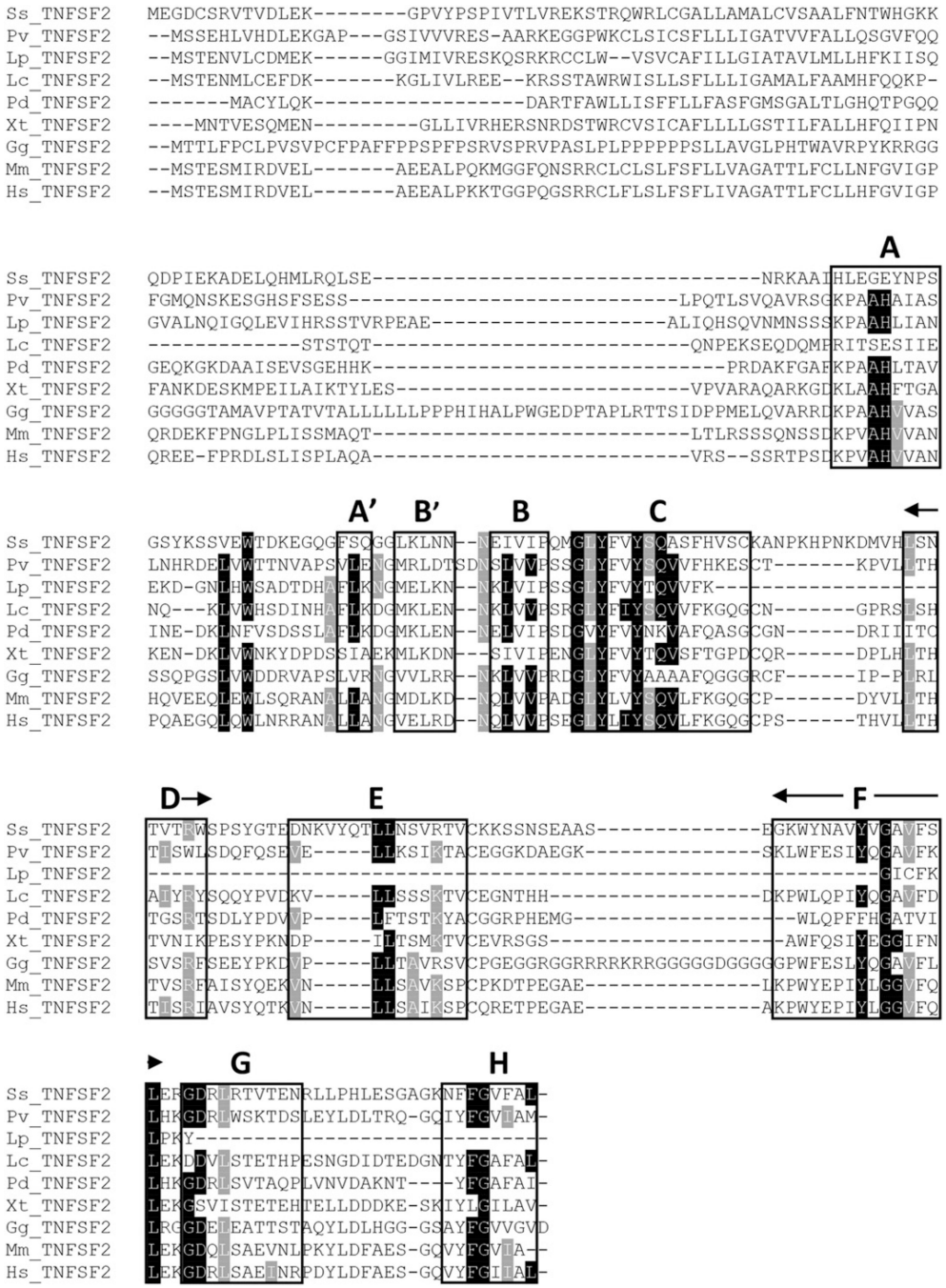

FIGURE 3.

TNFSF2 amino acid alignment. Boxes indicate amino acids that make up the β strand of the typical jelly roll fold for TNF family members. ighlighted in black are conserved amino acids in the THD. Black shading denotes the most conserved amino acids and gray denotes partially conserved amino acids. The black arrows are used to show the entire conserved domain when it did not fit on the same line. Bold letters denote a distinct subunit that makes up TNFSF2.

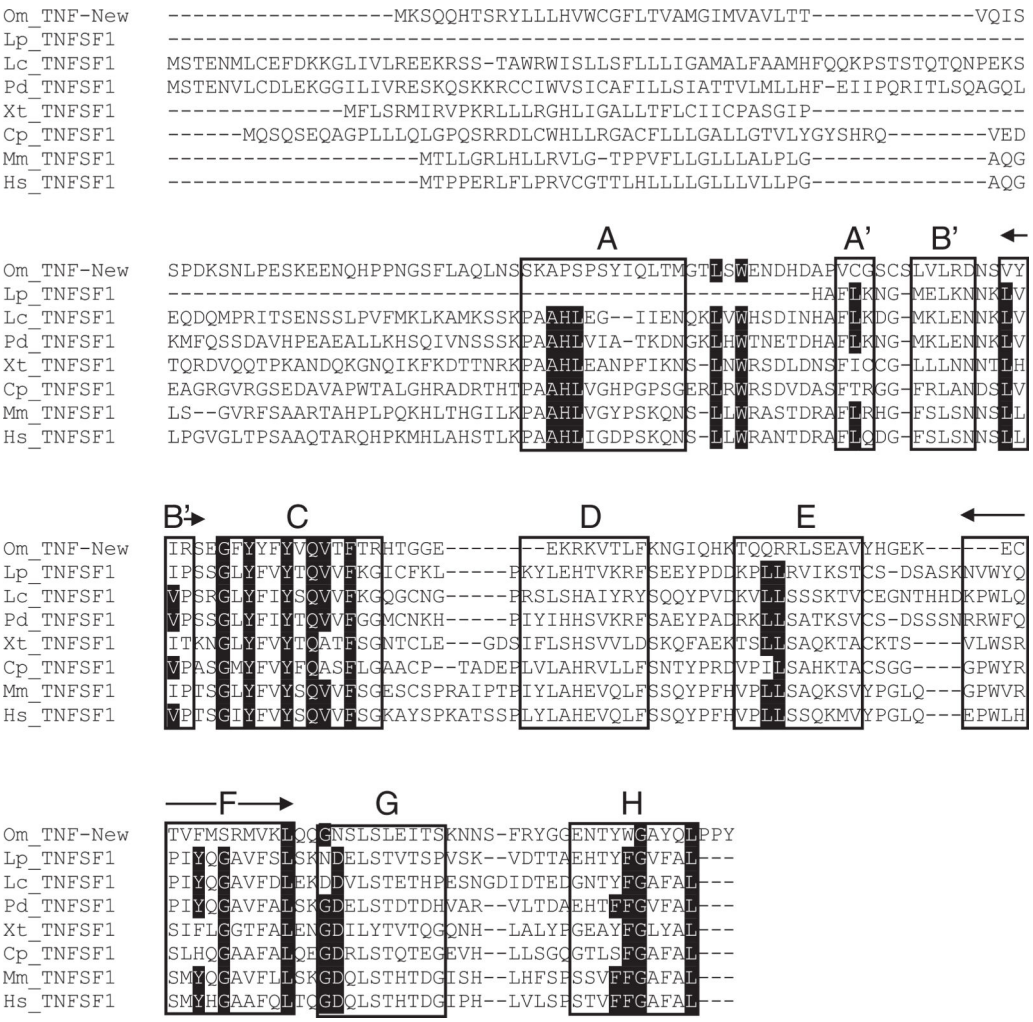

FIGURE 4.

TNFSF1 amino acid alignment. Boxes indicate amino acids that make up the β strand of the typical jelly roll fold for TNF family members. Highlighted in black are conserved amino acids in the THD. The black arrows are used to show the entire conserved domain when it did not fit on the same line. The black arrowheads denoted important amino acids that bind to TNFRSF3. Each bold letter denotes a distinct subunit that makes up TNFSF1.

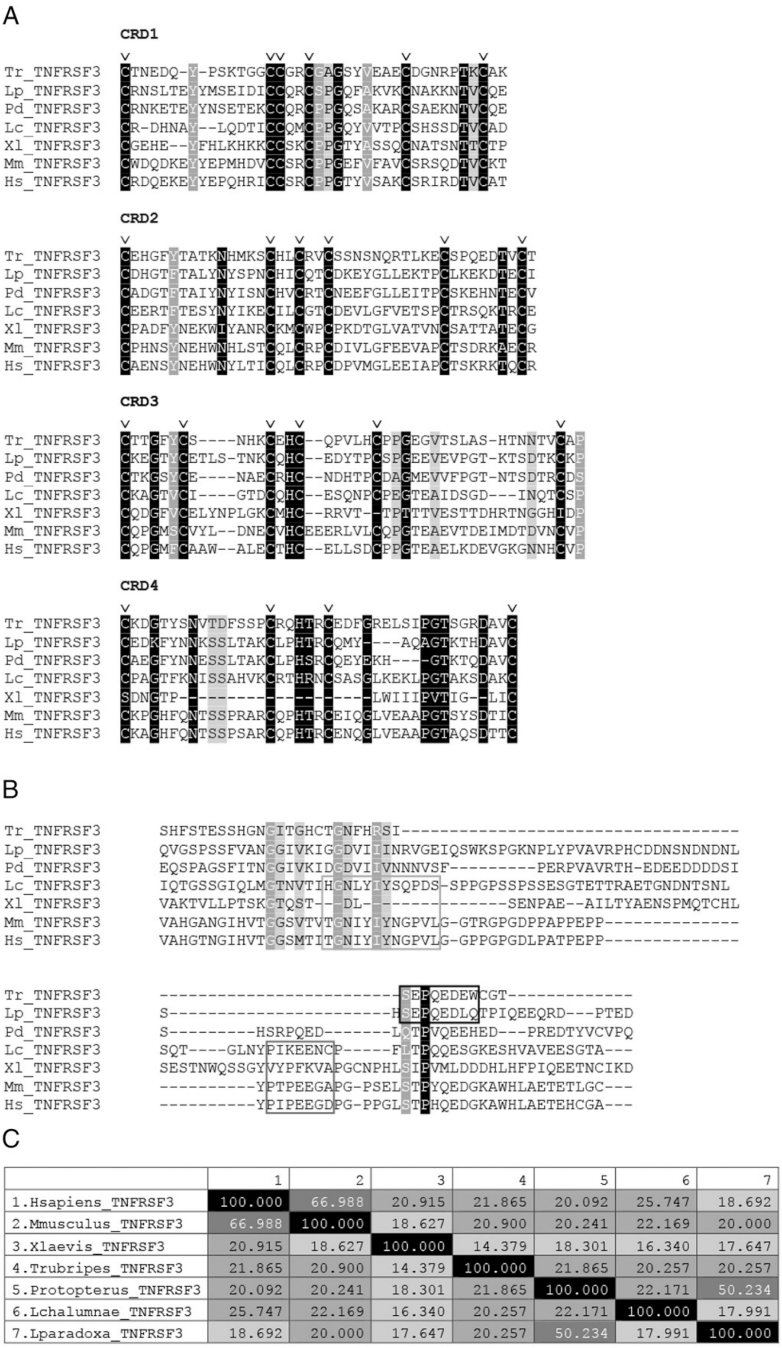

FIGURE 5.

Comparison of TNFRSF3 amino acid sequences among jawed vertebrates. (**A**) Extracellular domain of TNFRSF3, with triangles indicating extracellular CRD and residues required for ligand binding in mammals. (**B**) Alignment of TNFRSF3 intracellular domain. First box indicates unconventional TRAF binding motif, second box indicates conventional TRAF binding motif, and third box indicates a reported bony fish-specific conserved TRAF binding motif. (**C**) Amino acid sequence identity of TNFRSF3 molecules aligned in (A) and (B), darker shades of gray indicate higher percentage identity. The amino acids shaded in black,

dark gray, and light gray denote conserved amino acids going from most conserved to least conserved across vertebrate lineage, respectively. The “v” above certain columns indicates the conserved cysteines that denote the TNFRSF motif.

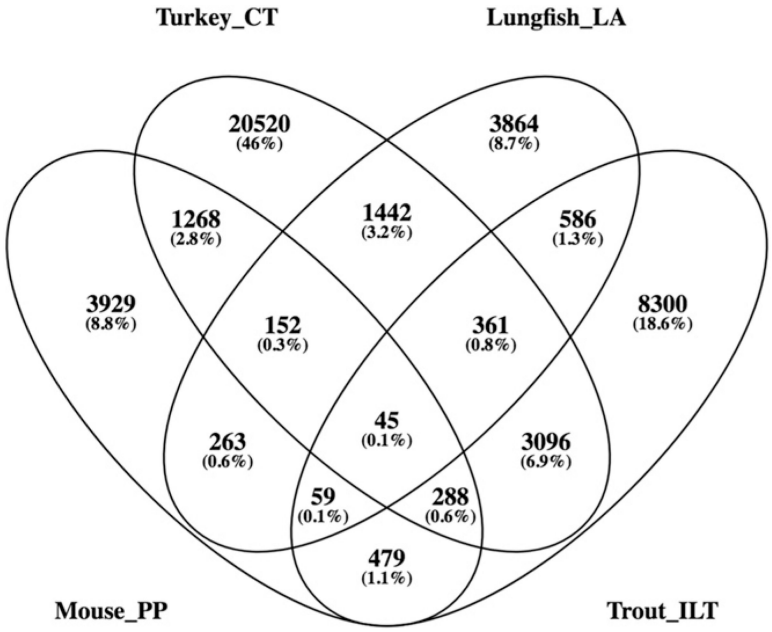

FIGURE 6.

Venn diagram of genes shared between different *O*-MALT transcriptomes generated in this study. Analysis was performed after removing genes found in control (non-*O*-MALT) tissues for each corresponding species.

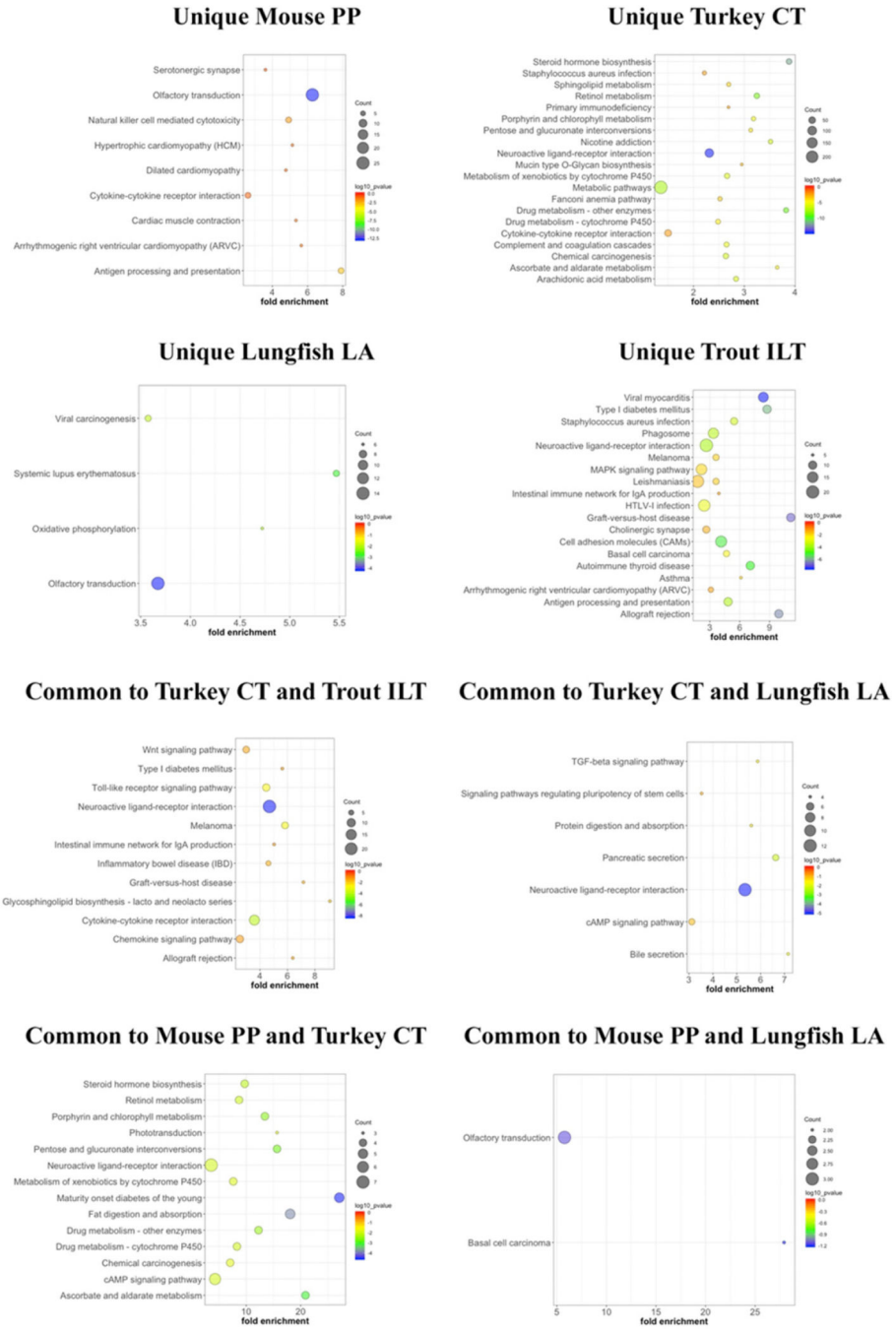

FIGURE 7.

Significantly enriched KEGG pathways from *O*-MALT transcriptomic data after removing genes expressed in corresponding negativecontrol (non-*O*-MALT) transcriptomes for each species.

Table I.

TNFSF ligands present in bony-jawed vertebrates

	TNFSF								
	Teleost	**Coelacanth**	**South American Lungfish**	**African Lungfish**	**Amphibian**	**Reptiles**	**Bird**	**Mouse**	**Human**
TNFSF1 (LTA)	−	+	+	+	+	+	−	+	+
TNFSF2 (TNF)	+	+	+	+	+	+	+	+	+
TNFSF3 (LTB)	−	+	+	+	+	−	−	+	+
TNFSF4	−	−	−	−	−	+	+	+	+
TNFSF5 (CD40LG)	+	+	+	+	+	+	+	+	+
TNFSF6 (FASLG)	+	+	+	+	+	+	+	+	+
TNFSF7 (CD70)	−	−	−	−	−	−	−	+	+
TNFSF8	−	+	−	+	−	+	+	+	+
TNFSF9	−	−	+	+[a]	−	+	−	+	+
TNFSF10	+	+	+	+	+	+	+	+	+
TNFSF11	+	+	−	+	+	+	+	+	+
TNFSF12	+	+	−	+	+	+	−	+	+
TNFSF13	+	+	+	+	+	+	−	+	+
TNFSF13B	+	+	+	+	+	+	+	+	+
TNFSF14	+	+	+	+	+	+	+	+	+
TNFSF15	+	+	−	−	−	+	+	+	+
TNFSF18	+	−	−	−	−	+	+	+	+
EDA-A1/EDA-A2	+	+	−	+	+	+	+	+	+
BALM	+	−	−	+	−	−	−	−	−
Ita/TNFN	+	−	−	−	−	−	−	−	−
Total number	14	14	10	15	12	16	12	18	18

Presence and absence of TNF ligands in all vertebrate classes. Only hits with an *E*-value lower than 1×10^{-5} were considered. Note that “presence” does not imply orthology with mammalian counterparts.

[a]Ligands that were not found through BLAST searches but were found using HMM searches. Only hits with an *E*-value lower than 1×10^{-5} were considered.

J Immunol. Author manuscript; available in PMC 2021 February 09.

Table II.

TNFRSF members present in bony-jawed vertebrates

	TNFRSF								
	Teleost	**Coelacanth**	**South American Lungfish**	**African Lungfish**	**Amphibian**	**Reptile**	**Bird**	**Mouse**	**Human**
TNFRSF1A	+	+	+	+	+	+	+	+	+
TNFRSF1B	+	+	+	+[a]	−	+	+	+	+
TNFRSF3 (LTBR)	+	+	+	+	+	−	−	+	+
TNFRSF4	+	+	+[a]	−	+	+	+	+	+
TNFRSF5 (CD40)	+	+	+	+	+	+	+	+	+
TNFRSF6 (FAS)	+	+	+	+	+	+	+	+	+
TNFRSF6B	+	+	−	−	+	+	+	+	+
TNFRSF7 (CD27)	+	+	−	+	−	−	+	+	+
TNFRSF8	+	−	+[a]	+[a]	+	+	+	+	+
TNFRSF9	+	+	+	+	+	+	+	+	+
TNFRSF10A	+	+	+	+	+	+	+	+	+
TNFRSF10B	+	+	+	−	+	+	+	+	+
TNFRSF10C	−	−	+	−	−	−	+	+	+
TNFRSF10D	−	−	−	−	−	−	−	−	+
TNFRSF11A	+	+	+	+	+	+	+	+	+
TNFRSF11B	+	+	+	+	+	+	+	+	+
TNFRSF12A	+	−	−	+[a]	+	+	+	+	+
TNFRSF13B	+	+	+	+	−	+	+	+	+
TNFRSF13C	−	−	+[a]	−	−	+	+	+	+
TNFRSF14	+	+	+	+	+	+	+	+	+
TNFRSF16 (NGFR)	+	+	−	+	+	+	+	+	+
TNFRSF17	+	+	+	+	+	+	+	+	+
TNFRSF18	+	+	−	−	−	+	+	+	+
TNFRSF19	+	+	−	−	+	+	+	+	+
TNFRSF19L (RELT)	+	+	−	−	+	−	+	+	+
TNFRSF21	+	+	+	+	+	+	+	+	+

	TNFRSF								
	Teleost	**Coelacanth**	**South American Lungfish**	**African Lungfish**	**Amphibian**	**Reptile**	**Bird**	**Mouse**	**Human**
EDAR	+	+	−	+[a]	+	+	+	+	+
TNFRSF25	+	+	−	−	−	+	+	+	+
TNFRSF27 (EDA2R)	−	+	−	−	+	+	+	+	+
Total number	25	24	18	18	21	24	27	28	29

Presence or absence of TNFRSF molecules in different vertebrate groups. BLAST and reverse-BLAST searches were performed using available transcriptomes and genomes from the main vertebrate groups. Only hits with an *E*-value lower than 1×10^{-5} were considered. Note that presence does not imply orthology with mammalian counterparts. TNFR superfamily members present in bony-jawed vertebrates.

[a]Sequences only found through HMM and not found through blasting the created transcriptomes.

Table III.

Percentage identity of TNFs between African lungfish and humans

Protein	Percentage Identity between *Protopterus* and Human
TNFSF1	**30.24**
TNFSF2	22.97
TNFSF3	27.63
TNFSF5	**32.95**
TNFSF6	**46.95**
TNFSF8	22.07
TNFSF9	19.57
TNFSF10	**39.15**
TNFSF11	**39.17**
TNFSF12	**48.05**
TNFSF13	27.80
TNFSF13B	**41.88**
TNFSF14	**37.31**
EDA	**81.92**
TNFRSF1A	26.84
TNFRSF1B	25.64
TNFRSF3	20.09
TNFRSF5	**30.69**
TNFRSF6	29.25
TNFRSF7	18.52
TNFRSF8	**30.71**
TNFRSF9	**29.80**
TNFRSF10A	19.51
TNFRSF11A	25.32
TNFRSF11B	**34.52**
TNFRSF12A	13.95
TNFRSF13B	**32.00**
TNFRSF14	27.92
TNFRSF16	**50.47**
TNFRSF17	24.32
TNFRSF21	**44.44**
EDAR	**64.79**

Percentage identity of TNF ligand and receptor sequences shared in humans and African lungfish, bold indicates higher percentage identity between lungfish and human sequences.

Table IV.

KEGG pathway analysis: enriched genes for the olfactory transduction pathway

Mouse PP	Lungfish LA	Mouse PP and Lungfish LA
6M1-16	OR10T2	CNGA3
OR11H4	OR13A1	OR52H1
OR14J1	OR4A16	OR52W1
OR1L4	OR52A1	
OR2G2	OR52A5	
OR2H1	OR52B2	
OR2L13	OR52B4	
OR2L2	OR52I1	
OR2L5	OR52I2	
OR2M4	OR52J3	
OR2M7	OR56A5	
OR2T10	OR5P2	
OR2T12	OR5P3	
OR2T29	OR9G9	
OR2T33		
OR2T5		
OR2T8		
OR4K5		
OR4P4		
OR52E6		
OR5D16		
OR5D18		
OR5L1		
OR5L2		
OR8B4		
OR8J1		

Genes within the olfactory transduction KEGG pathway found to be significantly enriched in lungfish LA and mouse PP transcriptomes.

Table V.

KEGG pathway analysis: enriched genes for the neuroactive ligand and receptor interaction pathway

Turkey CT			Trout ILT	Lungfish LA and Turkey CT	Turkey CT and Trout ILT	Mouse PP and Turkey CT
ADORA1	GRIK1	PLG	ADRA2A	CHRM2	ADORA3	CHRM1
ADORA2A	GRIK2	PTGDR	BDKRB2	CHRM4	AVPR1A	CHRM5
ADORA2B	GRIK3	PTGER1	C5AR1	DRD5	AVPR1B	GLP2R
ADRA1B	GRIK4	PTGER2	CCKAR	FSHR	AVPR2	NMUR1
ADRA1D	GRIK5	PTGER3	CHRNA1	GABRR2	C3AR1	NPBWR1
ADRB3	GRIN2A	PTGER4	CHRNA3	GPR35	CTSG	OPRL1
AGTR1	GRIN2B	PTGFR	CHRNA6	GPR83	CYSLTR1	TRHR
APLNR	GRIN2C	PTGIR	CHRNB1	GRIN1	GALR3	
BRS3	GRIN2D	PTH2R	GABBR1	HTR1B	GLRA1	
CALCR	GRIN3A	RXFP1	GABRQ	MC3R	GLRA2	
CALCRL	GRIN3B	RXFP2	GALR1	OPRD1	GLRA3	
CHRFAM7A	GRM5	RXFP4	GALR2	PRLHR	GLRB	
CHRM3	HRH2	S1PR4	GZMA		GPR156	
CHRNA7	HTR1D	SSTR2	HRH3		HTR1A	
CHRNA9	HTR1E	SSTR3	HRH4		HTR4	
DRD1	HTR2C	SSTR4	LTB4R2		HTR5A	
DRD2	HTR6	SSTR5	P2RY11		MC5R	
DRD3	HTR7	TAAR1	P2RY13		NPBWR2	
DRD4	LEPR	TACR1	P2RY14		NPFFR2	
F2	LTB4R	TACR2	PRLR		OXTR	
F2RL2	MC2R	TACR3			PTAFR	
F2RL3	MC4R	TBXA2R			UTS2R	
FPR2	MLNR	TSPO				
FPR3	MTNR1A					
FPRL1	MTNR1B					
FPRL2	NMDAR2C					
GABRA1	NMUR2					
GABRA2	NPFFR1					

J Immunol. Author manuscript; available in PMC 2021 February 09.

	Turkey CT	Trout ILT	Lungfish LA and Turkey CT	Turkey CT and Trout ILT	Mouse PP and Turkey CT
GABRA3	NPY1R				
GABRA4	NR2A				
GABRA5	NTSR1				
GABRA6	OPRK1				
GLP1R	OPRM1				
GRIA1	P2RY10				
GRIA2	P2RY6				
GRIA3	P2RY8				
GRIA4	PBR				

Significant genes involved in the neuroactive ligand and receptor interactions KEGG pathway found to be enriched in each *O*-MALT transcriptome or shared by two *O*-MALT transcriptomes.